CHAPTER ONE

INTRODUCTION

Renewable resources are clean or green energy sources that give much lower environmental impact than conventional energy sources. Renewable resources are attractive because they are replenished naturally, which means that they will never run out. Silicon is the most commonly used semiconductor in optoelectronic devices and Silicon photodiodes are extensively used in industrial applications as reliable devices for light to electricity conversion. Solar cells use the sun, a free and inexhaustible source of fuel, to produce emission-free electricity. In 2006, global cell production grew by 41% to 2520 MW. The crystalline silicon is the most important material in the photovoltaic today. According to predictions it will remain an important and dominant material in photovoltaic over the next 10-30 years; owing to its well recognized properties and its established production technology Crystalline silicon solar cells operate by absorbing light and using the discrete energy from the received photons to pump electrons to their exited state. The excited electrons migrate through the material's layers and produce an electrical current, there is no doubt that due to low production costs multicrystalline silicon is attractive substrate for solar cells. However, because of its worse electrical properties compared to monocrystalline silicon intense research is being performed to increase conversion efficiency of solar cells produced of multicrystalline silicon (Dobrzański & A. Drygała, 2008).

Cell efficiency depends on the silicon dopant, light density and wavelength, optical thickness and surface texture. Surface texturing, either in combination with an anti-reflection coating or by itself, can also be used to minimize reflection. Any "roughening" of the surface reduces reflection by increasing the chances of reflected light bouncing back onto the surface, rather than out to the surrounding air (Pveducation, 2015).

Laser processing is a very good technique for texturing silicon structures due to the contactless treatment. Moreover, textures of different patterns can easily be implemented on the treated surface without any additional masking. We have developed a method of laser texturing as a possible solution to the problem of surface textured silicon. Surface texture ensures that incident light meets the cell surface at least twice; transmission of light into the cell is thus considerably increased, the surface texture has many properties simultaneously, including very low reflectance at all incidence angles, and good light trapping that increases the optical path length inside the solar cell as shown in Figure (1.1)

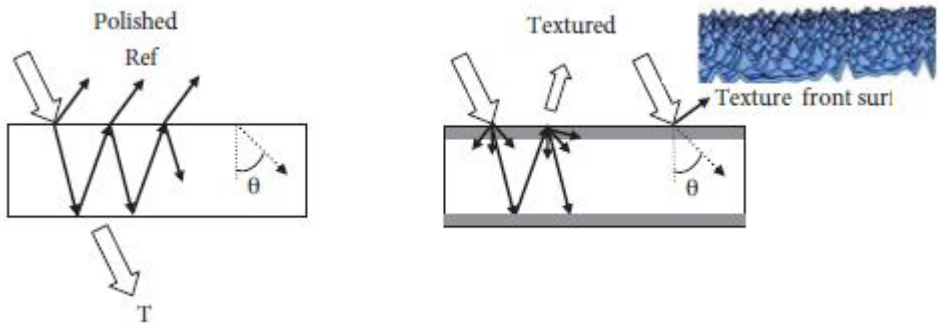

Fig (1.1): Texture decreases front surface reflectance for all wavelengths.

1-1 Study Objectives

This work aimed mainly to:

- Modify the surface of silicon solar cells using pulsed CO_2 laser.
- Use the Laser Direct Writing (LDW) method to get the texturing results.
- Investigation the effect of textured technique on the IV- characteristics curve and electrical properties of silicon solar cell.

1-2 Literature review

Dobrzański & A. Drygała in (2008) elaborated a laser method of texturization multicrystalline silicon. The main reason for taking up the research is that most conventional methods used for texturization of monocrystalline silicon are ineffective when applied for texturing multicrystalline silicon. This is related to random distribution

of grains of different crystalographic orientations on the surface of multicrystalline silicon.

In their work the topography of laser textured surfaces was investigated using ZEISS SUPRA 25 and PHILIPS XL 30 scanning electron microscopes and LSM 5 Pascal ZEISS confocal laser scanning microscope. The reflectance of produced textures was measured by Perkin-Elmer Lambda spectrophotometer with an integrating sphere. Electrical parameters of manufactured solar cells were characterized by measurements of I-V illuminated characteristics under standard AM 1.5 radiation. They found that a method of texturing of multicrystalline silicon surface using Nd: YAG laser appeared to be much more independent on grains crystallographic orientation compared to conventional texturing methods. Laser texturing makes it possible to increase absorption of the incident solar radiation. (Dobrzański & A. Drygała, 2008).

Taleb et al (2011) investigated and demonstrated the experimental evidence of the effect of femtosecond laser pulses on the spectral response of a silicon photovoltaic cell. The observed enhancement is related to the appearing of nano-structured grooves in the 700-900 nm range. The responsivity and the conversion efficiency of the photovoltaic cell are enhanced by this technique. Ultrashort laser pulses should be still economically reasonable in the large scale production. (Taleb et al 2011).

Kais A. Alnaimee in (2011), he utilized fast laser texturing technique to produce Micro/Nano surface textures in Silicon by means of UV femtosecond laser. He had prepared good absorber surface for photovoltaic cells. The textured Silicon surface absorbs the incident light greater than the non-textured surface. His results show a photovoltaic current increased about 21.3% in two dimensions laser textured area. (Kais A. Alnaimee, 2011)

Jostein Thorstensen and Sean Erik Foss (2011) in conference contribution, a process was developed for production of inverted pyramids and patch textures on (100) - oriented monocrystalline silicon for light-trapping. These textures have a high potential for light-trapping, but are normally produced by photolithography. The process described

in this paper is based on the use of a laser to create openings through an etch barrier, after which KOH etching of the underlying silicon develops a pattern consisting of (111) crystal orientations. The geometrical accuracy of the laser system is good, and the structures develop as intended, resulting in a texture with up to estimated 94 % area coverage.

D.A. Zuev et al in (2012) they performed experiments on the "black" mc-Si surface fabrication by the nanosecond pulses of the YAG laser second harmonic and on application of the introduced laser texturing method for the mc-Si solar cells efficiency improvement are represented. The developed version of laser texturing permits producing a low-reflection mc-Si surface with the reflectance of ~3% in the spectral range of 0.3-1 μm. The application of the introduced laser texturing method in mc-Si solar cells fabrication makes it possible to increase the short circuit current density and quantum efficiency. (D.A. Zuev et al, 2012)

Antanas VINČIŪNAS et al in (2013), they presented results of laser texturing of poly-Si solar cells surface by direct laser writing and novel Laser Beam Interference Ablation techniques. Texturing of the surface can increase the solar energy coupling within an active medium. Solar cells with laser-modified surface were characterized by optical and Raman spectroscopy as well as photo-electrically. After laser texturing of polycrystalline silicon solar cells, reflection from their surface was reduced by up to 14%. Structural defects induced by laser irradiation and ablation decreased the lifetime of photo-generated charge carriers and they could not reach the p-n junction. (Antanas VINČIŪNAS, 2013)

Jostein Thorstensen and Sean Erik Foss in (2013) in this paper, the light-trapping properties of the patch texture developed in PAPER I was investigated. Jo Gjessing (IFE) was of great assistance during the optical measurements. Optical absorption measurements on a patch textured silicon wafer are performed and these measurements are compared with ray-tracing simulations. This enables us to extract information about the quality of the texture. From these simulations, the current-

generating potential of the textures is extracted. It is found that the created texture gives an increase in I_{sc} of up to 0.5 mA/cm^2 compared to the random pyramids texture, and as such, it is concluded that it is possible to generate high quality textures with laser based methods. The process would be interesting for application on (100)-oriented monocrystalline silicon. It is recognized that the process must be simplified in order to justify the added process complexity. **(**Jostein Thorstensen and Sean Erik Foss .2013)

Marouf et al (2014) utilized a fast laser texturing technique to produce micro/nano surface textures in silicon by mean of UV femtosecond laser pulses. They demonstrated and investigated the experimental evidence of effect of femtosecond laser pulses on the spectral response of a silicon photovoltaic cell. And found that the use of this method leads to improve the responsivity and the conversion efficiency of the photovoltaic cell. The irradiation process leads to the formation of micro-nano meter periodic structure on substrates with a large area using single or double exposition. This technique is much cheaper and simpler than the electron beam lithography. (Marouf et al 2014).

Me in (2015) will Utilize laser surface texturing technique by using Infra red laser beam (Co_2 laser 10.6μm) that's produce molten points with 40 micron spaced to enhanced the reflection then increase the absorption of photons inside the conventional mono crystalline silicon solar cell.

1-3 Thesis Outlines

The thesis comprise of four chapters. Chapter one contains a short introduction to surface texturing and previous studies. The second chapter covers basics concepts and detailed theoretical background,; also contain the basics of the semiconductor solar cells, interaction of laser with silicon, application of laser in semiconductor material, and mechanism of laser surface texturing. The experimental part is fully described and presented in chapter three, a setup used to study the IV characteristic of the solar cell, also defines some material which used and each component with it is specifications. Then the results has been presented, analyzed and discussed in chapter four. Finally short

conclusions of this research and recommendations were presented for future works followed by list of Reference at the end of this chapter.

CHAPTER TWO
THEORETICAL BACKGROUND

The main task of photovoltaic is to reduce the cost of electricity produced by solar panels. The most obvious trend in the manufacture of solar cells is replacing most expensive technologies with new ones. That is why the investigations are currently being carried out to use the laser technologies in different stages of solar cells fabrication: creation of contact structures (laser scribing for buried contacts, laser-fired contacts, depth-selective laser ablation, and thin film selective removal), surface texturing to reduce reflection, deposition of transparent conductive oxides, laser doping, etc.

The application of laser radiation for crystalline silicon solar cells manufacture is especially prospective for the following reasons. The technologies of silicon solar cells production are almost perfected, and the struggle for fractions of a percent in their efficiency improvement is carried out. The silicon solar cells are the basis of photovoltaic power engineering and this state of affairs will remain in the near future. (D.A. Zuev, et al 2012).

2-1 Solar Cells Technology

A solar cell, or photovoltaic cell, is an electrical device that converts the energy of light directly into electricity by the photovoltaic effect, which is a physical and chemical phenomenon .(chemistryexplained 2015) It is defined as a device whose electrical characteristics, such as current, voltage, or resistance, vary when exposed to light. Solar cells are the building blocks of photovoltaic modules, otherwise known as solar panels.

Solar cells are described as being photovoltaic irrespective of whether the source is sunlight or an artificial light. They are used as a photo detector (for example infrared detectors), detecting light or other electromagnetic radiation near the visible range, or

measuring light intensity. Figure (2.1) shows a conventional crystalline silicon solar cell. Electrical contacts made from busbars (the larger strips) and fingers (the smaller ones) are printed on the silicon wafer. (Wikipedia 2015)

Fig (2.1): A conventional crystalline silicon solar cell. Electrical

2-1-1 Solar cell construction & Theory

The primary type solar cell that is constructed from a single crystal of silicon semiconductor. Silicon, chemical symbol (Si) is an abundant material on Earth. The Earth's crust is comprised of 25.7% silicon in its various forms. Silicon is may be found in sand, clay, granite, quartz, glass, cement and ceramics. It is the second most abundant element found on earth, after oxygen. Silicon must be highly purified (99.9999 %). Pure silicon does not conduct electricity; in fact it's an insulator. Each silicon atom has four electrons in its outer shell.

What makes silicon so useful in electronics is that by adding a small amount of impurities to the silicon while it is being manufactured alters its electrical properties in a very useful way. The impurities are called dopants in the industry, and the process of adding the impurities is called doping. One dopant material used is phosphorus. Phosphorus has five electrons in its outer shell. The free electron is a negative charge carrier and renders the silicon crystal electrically conductive and is called N-type silicon. Boron is another dopant. This element has only three electrons in its outer shell. The holes do render the silicon crystal conductive. The electron deficient silicon is called P-type silicon. When P-type and N-type silicon are placed in contact with one another it

forms a PN junction. A basic PN junction creates a diode that allows electricity to flow in one direction but not the other. Near the PN junction the electrons diffuse into the vacant holes in the P material causing a depletion zone. This depletion zone acts like an insulator preventing other free electrons in the N-type silicon and holes in the P-type silicon from combining.

A solar cell is essential a PN junction with a large surface area. The N-type material is kept thin to allow light to pass through to the PN junction.

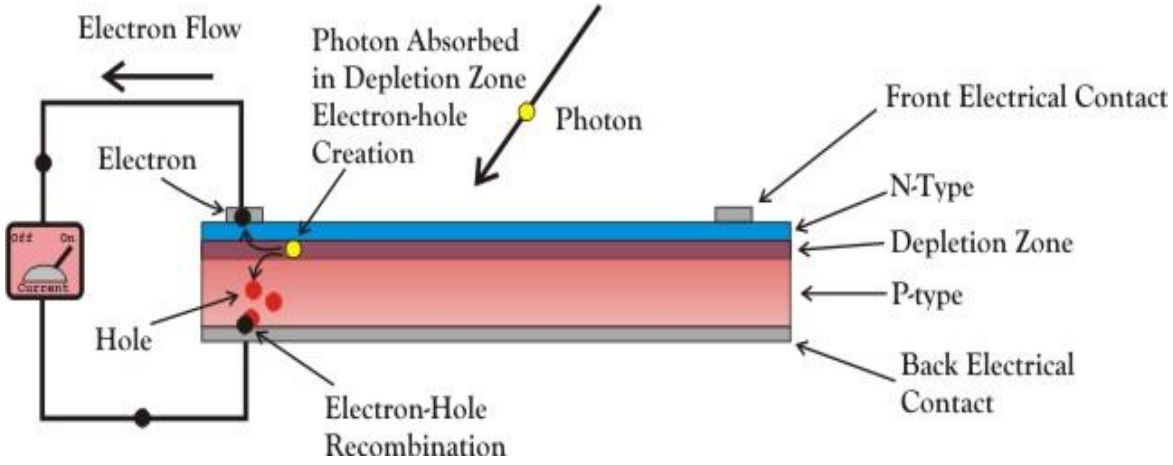

Fig (2.2): Solar cell Theory

Light travels in packets of energy called photons. The generation of electric current happens inside the depletion zone of the PN junction. The depletion region as explained previously with the diode is the area around the PN junction where the electrons from the N-type silicon, have diffused into the holes of the P-type material. When a photon of light is absorbed by one of these atoms in the N-Type silicon it will dislodge an electron, creating a free electron and a hole. The free electron and hole has sufficient energy to jump out of the depletion zone. If a wire is connected from the cathode (N-type silicon) to the anode (P-type silicon) electrons will flow through the wire. The electron is attracted to the positive charge of the P-type material and travels through the external load (meter) creating a flow of electric current. The hole created by the dislodged electron is attracted to the negative charge of N-type material and migrates to the back electrical contact. As the electron enters the P-type silicon from the back electrical

contact it combines with the hole restoring the electrical neutrality as showed in (figure 2.2). (Pveducation. 2015)

2-1-2 Optical properties of semiconductors

Photon absorption in semiconductor material strongly depends on the interaction between the incident photon flux and the electronic and lattice structures of the semiconductor. As the most important semiconductor material, silicon (Si) is a good example to illustrate the variations of optical properties of semiconductors in crystalline, polycrystalline, amorphous, and liquid forms. (Costas p.Grigoropoulos 2009).

Solar cells can be classified into first, second and third generation cells. The first generation cells also called conventional, traditional or wafer-based cells are made of crystalline silicon, which made of c-Si from wafers between 160 to 240 micrometers thick. The commercially predominant PV technology, that includes materials such as polysilicon and monocrystalline silicon which are made from cast square ingots large blocks of molten silicon carefully cooled and solidified. Second generation cells are thin film solar cells, that include amorphous silicon, CdTe and CIGS cells and are commercially significant in utility-scale photovoltaic power stations, building integrated photovoltaic's or in small stand-alone power system. The third generation of solar cells includes a number of thin-film technologies often described as emerging photovoltaic's most of them have not yet been commercially applied and are still in the research or development phase. Many use organic materials, often organometallic compounds as well as inorganic substances Organic and polymer solar cells are built from thin films (typically 100 nm) of organic semiconductors including polymers, such as polyphenylene vinylene and small-molecule compounds like copper phthalocyanine (a blue or green organic pigment) and carbon fullerenes. Energy conversion efficiencies achieved to date using conductive polymers are very low compared to inorganic materials.

Despite the fact that their efficiencies had been low and the stability of the absorber material was often too short for commercial applications, there is a lot of research invested into these technologies as they promise to achieve the goal of producing low-cost, high-efficiency solar cells.

2-1-3 Photovoltaic Effect

When the solar cell (p-n junction) is illuminated, electron–hole pairs are generated, and acted upon by the internal electric fields, resulting in a photocurrent (I_L). The generated photocurrent flows in a direction opposite to the forward dark current. Even in the absence of an external applied voltage, this photocurrent continues to flow, and is measured as the short-circuit current (I_{sc}). This current depends linearly on the light intensity, because absorption of more light results in additional electrons to flow in the internal electric field force. The overall cell current (I) is determined by subtracting the light induced current (I_L) from the diode dark current I_D.

Then;

$$I = I_D - I_L \ldots\ldots\ldots\ldots\ldots\ldots\ldots\ldots \quad (2.1)$$

$$I = I_0\left[\exp\left(\frac{eV}{kT}\right)-1\right] - I_L \ldots\ldots\ldots\ldots\ldots \quad (2.2)$$

This phenomenon is called the photovoltaic effect. (G. N. Tiwari and R. K. Mishra .2012).

2-1-4 Basic Parameters of Solar Cell

2-1-4-1 Overall Current (I)

This is determined by subtracting the light-induced current from the diode dark current and can be expressed as:

Overall current (I) = Diode dark current (I_D) - light induced current (I_L)

2-1-4-2 Short-Circuit Current (I_{sc})

This is the light generated current or photocurrent, I_L. It is the current in the circuit when the load is zero in the circuit. It can be achieved by connecting the positive and negative terminals by a copper wire.

2-1-4-3 Open-Circuit Voltage (V_{oc})

It is obtained by setting I=0 in expression for overall current, i.e. I=0 when $V=V_{oc}$. The open-circuit voltage is the voltage for maximum load in the circuit.

2-1-4-4 I–V Characteristics

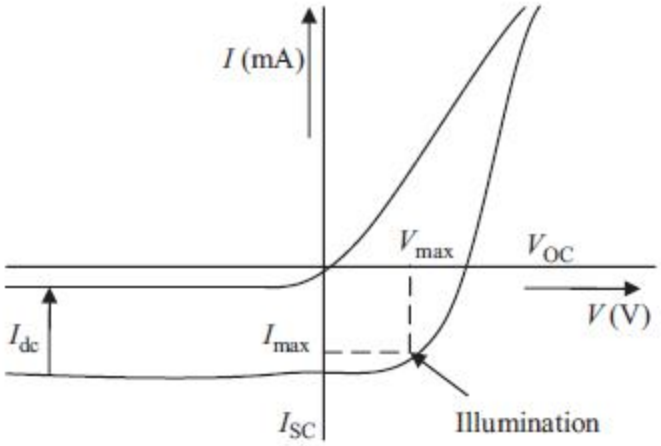

Fig (2.3): I–V characteristics of a solar cell with and without illumination.

The current equation for a solar cell is given by,

$$I = I_0\left[\exp\frac{e(V - IR_S}{kT} - 1\right] \text{..... (2.3)}$$

And is shown in Figure (2.3) for a good solar cell, the series resistance, R_s, should be very small and the shunt (parallel) resistance, R_p, should be very large. For commercial solar cells, R_p is much greater than the forward resistance of a diode so that it can be neglected and only R_s is of interest. The optimum load resistance R_L (P_{max}) = R_{Pmax} is connected, if the PV generator is able to deliver maximum power.

$$P_{max} = V_{pmax}\, I_{pmax} \text{..... (2.4)}$$

And $$R_{pmax} = V_{pmax} / I_{pmax} \text{..... .(2.5)}$$

The efficiency is defined as,

$$\eta = P/\Phi \quad \ldots\ldots\ldots\ldots\ldots\ldots\ldots\ldots\ldots\ldots \quad (2.6)$$

Where,

$P=V^{\times}I$, is the power delivered by the PV generator.

$\Phi=I_T{}^{\times}A_c$, is the solar radiation falling on the PV generator.

I_T is the solar intensity and A_c is the surface area irradiated.

2-1-4-5 Fill Factor (FF)

Another defining term in the overall behavior of a solar cell is the fill factor (FF). This is the available power at the maximum power point (P_m) divided by the open circuit voltage (V_{OC}) and the short circuit current (I_{SC}):

$$FF=\frac{P_m}{V_{oc}\times I_{sc}}=\frac{\eta\times A_c\times E}{V_{oc}\times I_{sc}} \quad \ldots\ldots\ldots\ldots\ldots\ldots \quad (2.7)$$

The fill factor, also known as the curve factor (Figure 2.4), is a measure of the sharpness of the knee in the I–V curve. It indicates how well a junction was made in the cell and how low the series resistance has been made. It can be lowered by the presence of series resistance and tends to be higher whenever the open-circuit voltage is high. The maximum value of fill factor is one, which is not possible. Its maximum value in Si is 0.88. (G. N. Tiwari and R. K. Mishra .2012)

$$FF=\frac{P_m}{V_{oc}\times I_{sc}}=\frac{I_{\max}\times V_{\max}}{V_{oc}\times I_{sc}} \quad \ldots\ldots\ldots\ldots\ldots\ldots \quad (2.8)$$

Cells with a high fill factor have a low equivalent series resistance and a high equivalent shunt resistance, so less of the current produced by the cell is dissipated in internal losses. At low light levels, the effect of the shunt resistance becomes increasingly important. As the light intensity decreases, the bias point and current through the solar

cell also decreases and the equivalent resistance of the solar cell may begin to approach the shunt resistance. When these two resistances are similar, the fraction of the total current flowing through the shunt resistance increases, thereby increasing the fractional power loss due to shunt resistance. Consequently, under cloudy conditions, a solar cell with a high shunt resistance retains a greater fraction of its original power than a solar cell with a low shunt resistance.

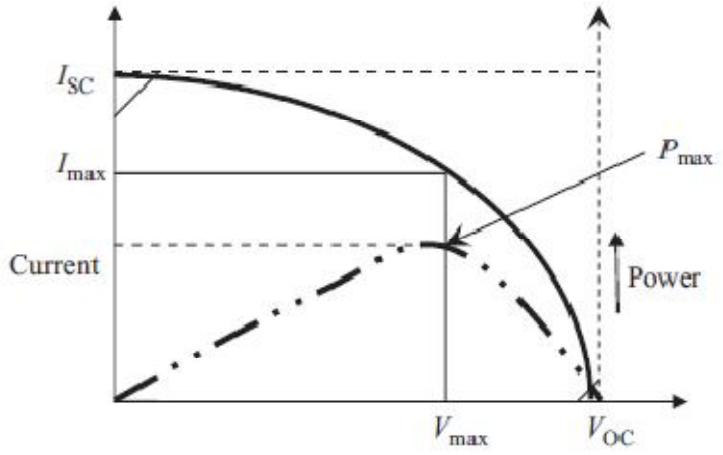

Fig (2.4); Characteristic and power curve for determining the fill factor (FF).

2-1-4-6 Maximum Power (Pmax)

No power is generated under short or open circuit. The power output is defined as,

$$P_{out} = V_{out} \times I_{out} \quad \ldots\ldots\ldots\ldots\ldots\ldots (2.9)$$

The maximum power Pmax provided by the device is achieved at a point on the characteristics, where the product IV is maximum. Thus,

$$P_{max} = I_{max} \times V_{max} \quad \ldots\ldots\ldots\ldots\ldots (2.10)$$

The maximum possible output can also be given as,

$$P_{max} = V_{oc} \times I_{sc} \times FF \ldots\ldots\ldots\ldots (2.11)$$

Where, FF is the fill factor given by Eq (2.8)

2-1-4-7 Solar Cell Efficiency (η_{ec})

It is the ratio of the electrical output of a solar cell to the incident energy in the form of sunlight. This is calculated by dividing a cell's power output (in watts) at its maximum power point (P_m) by the irradiance (input light), (I), in W/m^2 and the surface area of the solar cell (A_c in m^2).A solar cell has a voltage dependent efficiency curve, temperature coefficients, and allowable shadow angles.(Wikipedia 2015).

The solar cell power conversion efficiency can be given as;

$$\eta_{ec} = \frac{p_{\max}}{P_{in}} = \frac{I_{\max} \times V_{\max}}{incident..solar.radiation \times ..Area..of..solarcell} = \frac{V_{oc} \times I_{sc} \times FF}{I_{(t)} \times A_c} \quad \ldots\ldots (2.12)$$

Where, I_{max} and V_{max} are the current and voltage for maximum power, corresponding to solar intensity ($I_{(t)}$). Due to the difficulty in measuring these parameters directly, other parameters are substituted: thermodynamic efficiency, quantum efficiency (refers to the percentage of photons that are converted to electric current. Quantum efficiency is most usefully expressed as a spectral measurement (that is, as a function of photon wavelength or energy). Since some wavelengths are absorbed more effectively than others, spectral measurements of quantum efficiency can yield valuable information about the quality of the semiconductor bulk and surfaces), integrated quantum efficiency, V_{OC} ratio, and fill factor. Reflectance losses are a portion of quantum efficiency under "external quantum efficiency". Recombination losses make up another portion of quantum efficiency, V_{OC} ratio, and fill factor. Resistive losses are predominantly categorized under fill factor (G. N. Tiwari and R. K. Mishra .2012).

2-2 Interaction between lasers with matter

When light strikes the surface of a material, a portion will be reflected from the interface due to the discontinuity in the real index of refraction and the rest will be transmitted into the material. The fraction of the incident power that is reflected from the surface (R) depends on the polarization and angle of incidence (θ_i) of the light as well as the index of refraction of the atmosphere (n_1) and the material (n_2). The reflection

coefficients (R) are related to the transmission coefficients through T= 1- R, for the case of normally incident light on a flat surface.

$$R = \left(\frac{n_1 - n_2}{n_1 + n_2} \right)^2 \quad \text{……..(2.13)}$$

The reflectivity of a given material will depend on the frequency of the light source through the dispersion relation of its index of refraction. Also depend on the temperature of the material through changes in the permittivity, band structure, plasma oscillations, or material phase.

Once inside the material, absorption causes the intensity of the light to decay with depth at a rate determined by the material's absorption coefficient (α). In general, (α) is a function of wavelength and temperature, but for constant (α), intensity (I) decays exponentially with depth (z) according to the Beer–Lambert law.

$$I(z) = I_0 e^{-\alpha z} \quad \text{…… (2.14)}$$

Where ; I_0 is the intensity just inside the surface after considering reflection loss.

It is convenient to define the optical penetration or absorption depth, $\delta=1/\alpha$ which is the depth at which the intensity of the transmitted light drops to (1/e) of its initial value at the interface. Absorption depths are short relative to bulk material dimensions.

When dealing with CWor nanosecond duration laser pulses, it is typically assumed that most of the absorption is due to single photon interactions. However, for picoseconds (ps) and femtosecond (fs) lasers, the extremely high instantaneous intensity enables phenomena such as optical breakdown and multiphoton absorption which can significantly decrease absorption depths.

2-2-1 Relation between Reflectance, Transmission and Absorption

In general, reflection, transmission and absorption depend on the wavelength of the affected radiation. Thus, these three processes can either be quantified for monochromatic radiation. In addition, reflectance, transmittance and absorbance might

also depend on polarization and geometric distribution of the incident radiation, which therefore also has to be specified. The reflectance(R) is defined by the ratio of reflected radiant power to incident radiant power. The transmittance (T) of a medium is defined by the ratio of transmitted radiant power to incident radiant power. The absorbance (A) of a medium is defined by the ratio of absorbed radiant power to incident radiant power. Being defined as ratios of radiant power values

By Kirchhoff's radiation law, the flux emitted by a hot object must be equal to the amount absorbed by it; therefore, the emittance of an object must be equal to

$$A + R + T = 1 \quad \ldots\ldots\ldots\ldots\ldots\ldots (2.15)$$

As all light that is neither reflected nor transmitted must be absorbed the difference (1-R-T) is equal to the absorption (A). In a rough approximation we could now calculate the absorption coefficient (α) according to the equation:

$$R + T = e^{-\alpha d} \quad \ldots\ldots\ldots\ldots\ldots\ldots (2.16)$$

Where (d) is the thickness of the sample. (Grolik Benno, Kopp Joachim 2003)

Reflectance, transmittance and absorptance are dimensionless.

The optical properties of materials are not a constant since they are dependent on many parameters such as:

• Thickness of the sample

• Surface conditions

• Angle of incidence

• Temperature (Gigahertz-opitks,2015)

There are several key characteristics of the incident solar energy which are critical in determining how the incident sunlight interacts with a photovoltaic converter or any other object. The important characteristics of the incident solar energy are:

- The spectral content of the incident light.
- The radiant power density from the sun.
- The angle at which the incident solar radiation strikes a photovoltaic module.

The radiant energy from the sun throughout a year or day for a particular surface. (Pveducation 2015).

2-2-2 Energy Absorption Mechanisms

The specific mechanisms by which the absorption occurs will depend on the type of material. In insulators and semiconductors, the absorption of laser light predominantly occurs through resonant excitations such as transitions of valence band electrons to the conduction band (interband transitions) or within bands (intersubband transitions). These excited electronic states can then transfer energy to lattice phonons. Photons with energy below the material's band gap will not be absorbed (unless there are other impurity or defect states to couple to or if there is multiphoton absorption). Such energies typically correspond to light frequencies below vacuum ultraviolet for insulators and below the visible to infrared spectrum for semiconductors.

The time it takes for the excited electronic states to transfer energy to phonons and thermalize depends on the specific material and the specific mechanisms within the materials. For most metals, this thermalization time is on the order of 10^{-12}–10^{-10} s.
The spread in energy during the laser pulse combined with the spread in energy after the pulse can lead to changes in the material properties. The region over which these changes occur is denoted the heat affected zone (HAZ).

2-2-3 Material Response

Material responses that can occur in a material due to laser irradiation. These responses typically result in permanent changes to the material's surface chemistry, composition, crystal structure, and morphology. By choosing the appropriate laser parameters, precise control of the final material properties can be achieved.

2-2-3-1Thermally Activated Processes

Laser heating with fluencies below the threshold of melting can activate a variety of temperature dependent processes within the solid material. The high temperatures generated can enhance diffusion rates promoting impurity doping, the reorganization of

the crystal structure, and sintering of porous materials. The large temperature gradients achieved with localized laser heating can lead to rapid self-quenching of the material, trapping in highly non-equilibrium structures. Also, the rapid generation of large temperature gradients can induce thermal stresses and thermoelastic excitation of acoustic waves. These stresses can contribute to the mechanical response of the material such as work hardening, warping, or cracking.

2-2-3-2 Surface Melting

Flounces above the threshold of melting can lead to the formation of transient pools of molten material on the surface. The molten material will support much higher atomic mobility's and solubility's than in the solid phase, resulting in rapid material homogenization. High self-quenching rates with solidification front velocities up to several m/s can be achieved by rapid dissipation of heat into the cooler surrounding bulk material. Such rapid quenching can freeze in defects and supersaturated solutes as well as form metastable material phases. At temperatures far above the melting temperature, hydrodynamic motion can reshape and redistribute material.

2-2-3-3 Ablation

Laser ablation is the removal of material from a substrate by direct absorption of laser energy. Laser ablation is usually discussed in the context of pulsed lasers; however, it is also possible with intense CW irradiation. The onset of ablation occurs above a threshold flounce, which will depend on the absorption mechanism, particular material properties, microstructure, the presence of defects, and on laser parameters such as wavelength and pulse duration.

A combination of ablation, surface melting, and thermally activated processes, which can lead to cumulative changes in the material's surface texture, morphology, and chemistry. For instance, residual heat left after ablating material from a surface can lead to further melting or other thermally activated processes in the remaining surface and surrounding volume of material. These collective effects can result in complex Multiscale material modifications.

2-2-4 Interaction between Laser and Silicon

After the absorption of short laser pulses of high peak intensities silicon is heated up so that the surface is partially molten. If the absorbed energy is sufficiently high some of the material is explosively evaporated from the molten layer. The recoil pressure of evaporated material and the plasma plume formed in this process ejects a part of molten layer. As a result of this violent expulsion of the material the deposition of solidified silicon droplets, both inside and outside of the groove can be observed Bottom and sidewalls of laser scribed grooves are covered with molten, not evaporated and resolidified material. Solar cells manufactured from laser textured wafers that were not etched shown very low conversion efficiency .It was a result of detrimental influence of laser induced defects on the operation of solar cells. Therefore, post laser processing etching was performed to remove laser damaged layer. With the increase of thickness of removed layer positive ridges were etched off and textured surface was smoothened away. Furthermore, the angle between sidewalls increased resulting in formation of so-called V-grooves. In the bottom of the grooves may be observed regions of regular shape dependent on crystallographic orientation of substrate. As a result of laser processing and subsequent etching texture of uniform structure were obtained Solar cells manufactured from laser textured wafer that were not etched demonstrating extremely low efficiency. This is the result of damages introduced into the top layer of the material during laser texturing. These damages have detrimental influence on the operation of solar cell and reduce its performance mainly through increased recombination and/or junction shunting. Fortunately, it appears that detrimental influence of laser induced damage on the solar cells performance may be successively mitigated by post laser processing etch procedure. Applied etching step enable to remove layer of laser induced defects from the textured surface. Many trials have been performed to adjust etch concentration and thickness of removed layer. It can be observed that with the increase of thickness of removed layer efficiency of solar cell grows but at the same time the effective reflectance increase as well. Consequently, post-laser texturing etching

improves electrical properties of textured material but deteriorates its optical properties. That is why the proper adjustment of thickness of removed layer must be a trade of balancing these properties of solar cells. (Dobrzański & A. Drygała, 2008).

2-3 Laser Surface Modification

Lasers provide the ability to accurately deliver large amounts of energy into confined regions of a material in order to achieve a desired response. For opaque materials, this energy is absorbed near the surface, modifying surface chemistry, crystal structure, and/or Multiscale morphology without altering the bulk. Modification of surface properties over multiple length scales plays an important role in optimizing a material's performance for a given application. For instance, the cosmetic appearance of a surface and its absorption properties can be controlled by altering its texture and presence of chemical impurities in the surface. Confinement of deposited energy to desired regions on a material's surface can be achieved by controlling the laser's spatial intensity profile. The predominant methods for control include beam steering by fixed or galvanometric scanning mirrors, beam focusing through telescoping or converging optics, and beam shaping with homogenizers, amplitude masks, refractive elements, and diffractive optical elements (DOE). (Matthew S. Brown and Craig B. Arnold 2010)

2-3-1 Surface Texturing for Enhanced Optical Properties

In this case study, discuss how laser texturing of semiconductor surfaces can be utilized to capture as much of the incident light as possible. To decrease reflections and increase absorption for enhanced device performance without altering bulk properties.

Light enters through the air–material interface, where a discontinuity in the index of refraction causes a portion of the wave to reflect and carry off a fraction of the incident power equal to the reflectivity (Eq 2.13). Because of the high index of refraction of most semiconductors, this parasitic Fresnel reflection (e.g., 30% for silicon and 25% for CdTe) can significantly reduce the optical power available for transduction into an electrical response. The most common solution is to apply a single-layer, thin-film antireflection coating; however, such coatings are effective only in a narrow spectral

range and at normal incidence. Broadband reduction in reflectivity over a larger range of incidence angles can be achieved with multilayer and graded index (GRIN) thin films. However, their application tends to be costly and the availability of coating materials with the appropriate physical and optical properties is limited.

An alternative method for the reduction of reflections is to texture the existing semiconductor surface. Because no additional material is added, these textured surfaces are inherently more stable and do not suffer from material compatibility issues that plague thin films such as weak adhesion, thermal expansion mismatch, and interdiffusion. Multiscale texturing of a surface can cause significant deviations in how light is reflected and scattered, leading to enhanced absorption over that of a flat smooth surface. For surface features with dimensions greater than several wavelengths of light, this enhancement can most easily be described using the principles of ray optics. A portion from a ray of light will specularly reflect from a flat surface, and have no further interaction with the material. On the other hand, protruding features can reflect and scatter light back onto the surface; Light can effectively become trapped in crevices and holes where multiple reflections enhance the coupling into the material. Once inside these protruded structures, multiple internal reflections can guide the light into the bulk. Refraction at the surface of these structures also leads to transmission at oblique angles, effectively increasing the optical path length, enhancing absorption. The degree of enhancement depends on the particular geometry and dimension of the surface features. The creation of features at or near the surface with dimensions on the order of a wavelength (e.g., cracks, voids, and surface roughness) can also affect the surface reflectivity by scattering light in the material and increasing the optical path length, leading to enhanced absorption. This is especially important for enhancing absorption in thin-film devices where the thickness of the film is on the order of the optical wavelength. Light trapping is usually achieved by changing the angle at which light travels in the solar cell by having it be incident on an angled surface. A textured surface will not only reduce reflection. Also couple light obliquely into the silicon like Fig (2.5)

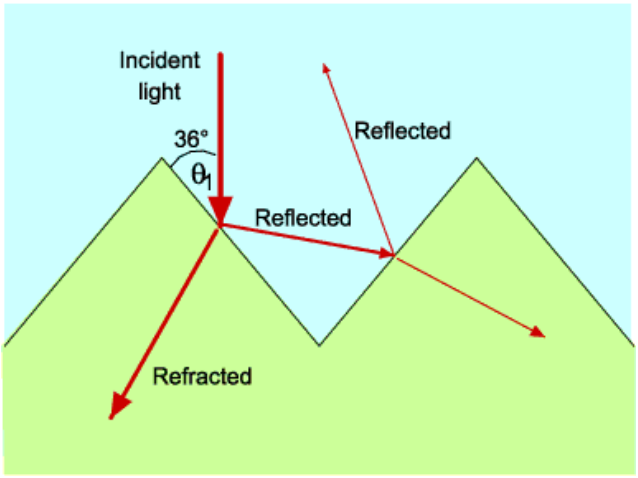

Fig (2.5): Reflection and transmission of light for a textured silicon solar cell.

Thus giving a longer optical path length than the physical device thickness. The angle at which light is refracted into the semiconductor material is, according to Snell's Law, as follows:

$$n_1 \sin\theta_1 = n_2 \sin\theta_2 \quad \text{.....(2.17)}$$

Where θ_1 and θ_2 are the angles for the light incident on the interface relative to the normal plane of the interface within the mediums with refractive indices n_1 and n_2 respectively. θ_1 and θ_2

By rearranging Snell's law above, the angle at which light enters the solar cell (the angle of refracted light) can be calculated:

$$\theta_2 = \sin^{-1}(n_2 n_1 \sin\theta_1) \quad \text{.....(2.18)}$$

In a textured single crystalline solar cell, the presence of crystallographic planes make the angle θ_1 equal to 36°.

The amount of light reflected at an interface is calculated from the Fresnel reflection formula. For light polarized in the parallel to the surface the amount of reflected light is:

$$R_{//} = \tan^2(\theta_1 - \theta_2)\tan^2(\theta_1 + \theta_2) \qquad (2.19)$$

Using total internal reflection, light can be trapped inside the cell and make multiple passes through the cell, thus allowing even a thin solar cell to maintain a high optical path length.

While the reduction of reflection is an essential part of achieving a high efficiency solar cell, it is also essential to absorb all the light in the silicon solar cell. The amount of light absorbed depends on the optical path length and the absorption coefficient. (Bunea G, et al. 2006)

There are many different kinds of texturization techniques to modify the solar cell surface for trapping of the incident light:

Acid texturization is the creation of randomly distributed pyramids by direct chemical etching based on HNO3: HF solutions. As the etching rate differs in various crystallographic directions, a pyramidal structure can be formed in mono-crystalline silicon solar cells. One such pyramid is illustrated in the drawing below Fig (2.6). An electron microscope photograph of a textured silicon surface is shown in the photograph below Fig (2.7) Image Courtesy of the School of Photovoltaic & Renewable Energy Engineering, University of New South Wales.(Bailey, W.L. et al, 1979).

Unfortunately, this technique cannot work effectively on polycrystalline silicon wafers. On the other hand, alkali etching can cause undesirable fractures on the surface of the polycrystalline silicon solar cell.

There is another ways like: mechanical etching using diamond Edge, reactive ion etching and plasma etching have been proposed. All of them have limitations in size and aspect ratio of texturing. And have some advantages and drawbacks.

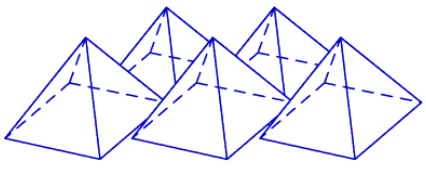

Fig (2.6): A square based pyramid which forms the surface of an appropriately textured crystalline silicon solar cell.

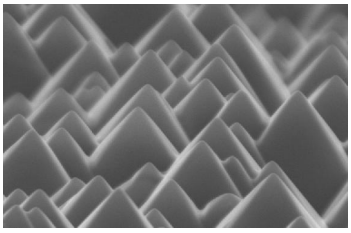

Fig (2.7): SEM photograph of a textured silicon surface.

The application of etches based on HF-HNO_3 induces difficult reproducible results due to random distribution of grains of different crystallographic orientation on the surface of multicrystalline silicon and necessity of precise control of temperature as well as composition of etches. Reactive ion etching creates a needle-like surface, on which screen printing is difficult, but this problem can be overcome by an additional wet chemical etching step. However, the additional alkaline etching step brings the disadvantage of a reduced gain in reflectance. Mechanical texturing may be effective, but has some limitations related to textured material. It cannot be applied specially for thin, warped, and fragile materials. (Dobrzański & A. Drygała, 2008).

The other novel methods for texturing polycrystalline silicon (poly-Si) solar cells use laser ablation .Lasers can produce surface structures which are able to trap photons. PV efficiency of c-Si solar cells was increased by 2% when nano-hole matrixes were formed by a laser in anti-reflective Si_3N_4 coating. The effective area of silicon solar cells was increased by texturing silicon substrate using laser ablation with beam interference The laser processing is very promising technique for texturing multicrystalline silicon due to the contactless treatment. Moreover, texture of different patterns can easily be implemented on the treated surface without any additional masking. Successive grooves were scribed with constant spacing within consecutive scanning the wafer surface by laser beam in the opposite directions. Many trials for different values of laser parameters were carried out.

There are two distinct methodologies which have been investigated for laser texturing surfaces to enhance absorption.

The first is direct-write micromachining where a focused beam is scanned across a surface in a pattern to selectively ablate material and define the structures It has been

used to texture pits, grooves, and pyramidal structures in mono and polycrystalline silicon to enhance absorption . Laser direct write allows a great deal of flexibility in defining surface texture; however, feature dimensions are limited by the focus size of the beam.

The second laser texturing methodology is based on spontaneously forming quasi-periodic microstructures, which have been observed on laser exposed surfaces. Under the right conditions, arrays of high-aspect-ratio features such as cones or pillars will fill the irradiated regions of the surface. Surfaces textured in this manner exhibit some of the highest increases in absorptance over a wider spectral band than surfaces textured by the other techniques. And unlike direct writing, large areas can be textured at once by using an unfocused beam.

Therefore, there has been a lot of interest in understanding how these structures form and their dependence on processing parameters in order to optimize the processing for cost effective integration into the commercial mass production of semiconductor devices. Irradiation with a higher flounce near or above the ablation threshold, such as that during pulsed-laser deposition, has been found to lead to surface roughening with larger scale features such as mounds or small mountains (Matthew S. Brown and Craig B. Arnold 2010)

Different patterns can be used; the common microstructures are linear grooves, crossed grooves, and circular dimple-like depressions (Figure 2.8) shows a magnified image of patterned hemispherical depressions created with laser surface texturing on a materials surface.

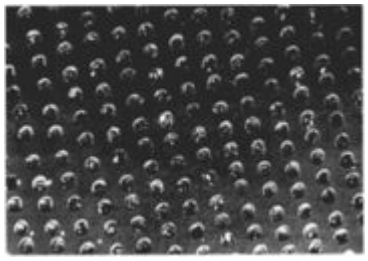

Figure (2.8): Magnified image of patterned hemispherical depressions

In order to manufacture pattern surface microstructures, the laser used needs to be suitable for the workpiece material and capable of either melting or ablating the material. In practice, some of the main types of lasers utilized in LST are Nd: YAG laser, carbon dioxide laser, and excimer lasers. The lasers are usually pulsed, often using a Q-switching setup , to produce one dimple per pulse. With high repetition rates (pulse durations of μm to fs), thousands of dimples can be created in very short processing times. With possible speeds of well over 1000 microcavities produced per second, LST can be scaled to large areas.

Nd: YAG and CO_2 are more common than excimer lasers, as excimer lasers have comparatively low ablation rates and take excessive time for LST. On the other hand, due to the low abolition of excimer lasers, they can be used to create microstructures within micrometer precision. As well, excimer lasers are often used with lithography methods and etching procedures to create surface textures.

Cutting and removal rates depend on the laser power, wavelength, pulse duration, and on the material properties of the workpiece; characteristics such as absorption, thermal conductivity, and thermal capacity. The hardness of the material does not affect its laser cutting rate, making LST effective on typically difficult substances like carbides and ceramics. (Appropedia, 2015)

2-3-2 Laser Direct-Write Processing

Direct-write techniques enable computer controlled two and three dimensional Pattern formation in a serial fashion. Among these techniques, the versatility offered by laser based direct-write methods is unique, given their ability to add, remove, and modify different types of materials without physical contact between a tool or nozzle and the material of interest. Laser pulses used to generate the patterns can be manipulated to control the composition, structure, and even properties of individual three-dimensional volumes of materials across length scales spanning six orders of magnitude, from nanometers to millimeters. Such resolution, combined with the ability to process complex or delicate material systems, enables laser direct-write tools to

fabricate structures that are not possible to generate using other serial or parallel fabrication techniques.

In general, direct-write processing refers to any technique that is able to create a pattern on a surface or volume in a serial or “spot-by-spot” fashion. This is in contrast to lithography, stamping, directed self-assembly, or other patterning approaches that require masks or preexisting patterns.

The key elements of any LDW system can be divided into three subsystems:

Laser source, (2) beam delivery system, and (3) substrate/target mounting system. (Figure 2.9) shows an Schematic illustration of a laser direct-write system. The basic components of an LDW system are (left to right) a substrate mounting system, a beam delivery system, and a laser source. Motion control of either the beam delivery system or the substrate mounting system is typically accomplished using computer-assisted design and manufacturing (CAD/CAM) integrated with the laser source.

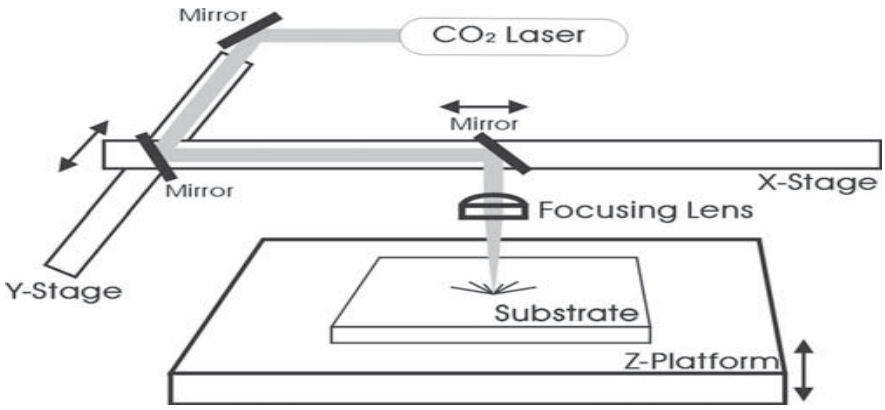

Fig (2.9): Schematic illustration of a laser direct-write system.

2-3-3 Direct Beam, Scanning, and Interference Patterns

In order to produce the patterned microstructures on the material’s surface, the laser beam position relative to the surface has to be manipulated. There are three main techniques for controlling the laser ablation to create the desired patterns: Direct beam movement, scanning, and the use of interference patterns. The technique to be used depends on the workpiece geometry, the scale of production, and the budget.

2-3-3-1 Direct Beam

The direct beam methodology applies the laser beam directly to the material's surface. An ablation head focuses the laser and a high pressure gas line blows away melted and sublimated material. A mechanized system allows for the workpiece or the ablation head to be moved in controlled increments. By manipulating the relative position of the ablation head and the workpiece, along with the pulse duration of the laser, the frequency of surface depressions can be controlled.

2-3-3-2 Scanning

Another method of controlling the laser patterning is to utilize a scanning system. By reflecting the laser beam with a series of motorized mirrors, the laser beam can be quickly moved to the desired position for each microcavity to be created. These motorized mirrors, usually referred to as a mirror galvanometer, can precisely and rapidly direct the laser beam to the desired contact point. To ensure the beam does not strike the surface on an angle, a flat field lens is utilized to ensure the beam and surfaces are perpendicular at the contact point. (Appropedia .2015)

2-3-3-3 Interference Patterns

To create patterned grooves and crossed grooves, optical interference patterns can also be used. The interference pattern covers the size of the beam diameter and creates many microcavities at once. When two beams interfere with each other, constructive and destructive interference occur, creating parallel linear lines of light. If this pattern of laser light is directed at a material's surface for a given time, ablation and melting will occur, creating parallel linear grooves. The period of the linear grooves is given by the formula:

$$\text{Period} = \lambda / (2\sin(\alpha/2)) \quad \ldots\ldots\ldots\ldots\ldots \quad (2.20)$$

Where: λ is the laser wavelength, α is the angle between the laser beams. To create a crossed groove microstructure, a sample can be exposed in one orientation to create

linear grooves, and then rotated 90° and exposed again to the light to create crossed grooves.

2-3-3-4 Pore Geometry, Size, and Frequency

The optimum patterning and geometry of microspores for the best tribological characteristics depend on several application factors and is not an exact science. With dimple-like depressions, it is found that the exact geometry is not significant compared to the ratio between pore diameter and depth, and the area fraction covered by pores. The application factors that influence the optimum pore ratio and area fraction include: Load capacity, Pressure, Material Sliding and Velocity. (Appropedia 2015).

2-3-4 LDW laser Source

Laser used for LDW process in this work are Carbon Dioxide Laser.

2-3-4-1 Carbon Dioxide laser:

The carbon dioxide laser (CO_2 laser) was one of the earliest gas lasers to be developed (invented by Kumar Patel of Bell Labs in 1964), and is still one of the most useful. Carbon dioxide lasers are the highest-power continuous wave lasers that are currently available. They are also quite efficient the ratio of output power to pump power can be as large as 20%. The CO_2 laser produces a beam of infrared light with the principal wavelength bands centering around 9.4 and 10.6 micrometers. The active laser medium (laser gain/amplification medium) is a gas discharge which is air cooled. The filling gas within the discharge tube consists primarily of:

- Carbon dioxide (CO_2) (around 10–20%)
- Nitrogen (N_2) (around 10–20%)
- Hydrogen (H_2) and/or xenon (Xe)(a few percent; usually only used in a sealed tube)
- Helium (He) (The remainder of the gas mixture)

Because CO_2 lasers operate in the infrared, special materials are necessary for their construction. Typically, the mirrors are silvered, while windows and lenses are made of either germanium or zinc selenide. For high power applications, gold mirrors and zinc selenide windows and lenses are preferred. The CO_2 laser can be constructed to have CW powers between milliwatts (mW) and hundreds of kilowatts (kW). It is also very easy to actively Q-switch a CO_2 laser by means of a rotating mirror or an electro-optic switch, giving rise to Q-switched peak powers of up to gigawatts (GW).
(Wikipedia 2015)

Pumping in the CO_2 laser occurs directly by electron impact and by collision with vibrationally excited N_2. The CO_2 laser discharge is normally operated in a mixture of (CO_2, N_2, and He) gas at pressures of up to 1 atm. Relative concentrations of the three gas components must be chosen to optimize emission in a particular device.

In a CO_2 laser one uses the transitions occurring between different vibrational states of the carbon dioxide molecule. Figure (2.10) shows the carbon dioxide molecule consisting of a central carbon atom with two oxygen atoms attached one on either side. Such a molecule can vibrate in the three independent modes of vibration these correspond to the symmetric stretch, the bending, and the asymmetric stretch modes. Each of these modes is characterized by a definite frequency of vibration. According to basic quantum mechanics these vibrational degrees of freedom are quantized, i.e., when a molecule vibrates in any of the modes it can have only a discrete set of energies. Thus if we call v_1 the frequency corresponding to the symmetric stretch mode then the molecule can have energies of only

$$E = \left(m + \frac{1}{2} \right) h\nu \qquad \text{m=0, 1, 2} \quad \ldots\ldots\ldots\ldots\ldots\ldots\ldots \quad (2.21)$$

When it vibrates in the symmetric stretch mode. Thus the degree of excitation is characterized by the integer m when the carbon dioxide molecule vibrates in the symmetric stretch mode. In general, since the carbon dioxide molecule can vibrate in a

combination of the three modes the state of vibration can be described by three integers (mnq).

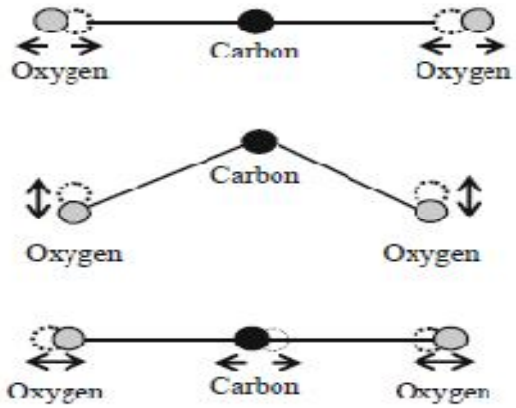

Fig.(2.10): The three independent modes of vibration of the carbon dioxide molecule

The three integers correspond, respectively, to the degree of excitation in the symmetric stretch, bending, and asymmetric stretch modes, respectively. Figure (2.11) shows the various vibrational energy levels taking part in the laser transition. Energy transfer from excited nitrogen molecules to carbon dioxide molecules results in the excitation of carbon dioxide molecules. Important lasing transitions occur at 9.6 and 10.6 μm. The laser transition at 10.6 μm occurs between the (001) and (100) levels of carbon dioxide. The excitation of the carbon dioxide molecules to the long-lived level (001) occurs both through collisional transfers from nearly resonant excited nitrogen molecules and also from the cascading down of carbon dioxide molecules from higher energy levels. Electrical pulsing can be used to obtain trains of millisecond or microsecond pulses with peak powers that are - 10^2 larger than the CW power. Electro-optical or acousto-optical intracavity modulation can be used with CW CO_2 lasers to produce trains of nanosecond pulses with peak power of 10 kW. Operation under axial flow conditions at low pressure (l0-50 torr) typically yields output powers of 50-100 W m^{-I} with the larger value being obtained with shorter tubes.

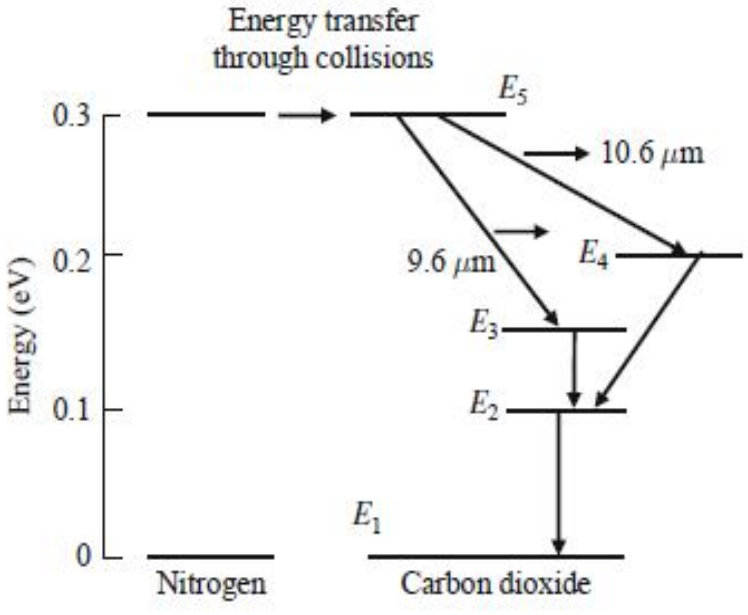

Fig. (2.11): The vibrational levels of nitrogen and carbon dioxide molecules

The reduction in the power per unit length factor that occurs with an increase in tube length makes it unattractive to increase tube length beyond about 10m. Higher CW laser powers can be obtained in axial flow configurations by an increase in gas pressure and gas flow rate. This results from a change to convective gas cooling from the diffusive cooling that ordinarily occurs in low pressure, low-flow devices. An example of the advantages of fast axial flow can be seen in the 2kW. An output of up to 2 kW is obtained from 4 m of discharge tube. This represents a power per unit length ratio of 500 W m^{-I}.

The CO_2 laser possesses an extremely high efficiency of ≈30%. This is because of efficient pumping to the (001) level and also because all the energy levels involved are close to the ground level. Thus the atomic quantum efficiency which is the ratio of the energy difference corresponding to the laser transition to the energy difference of the pump transition, i.e.,

$$\eta = \frac{E_5 - E_4}{E_5 - E_1} \qquad (2.22)$$

Where:

η is atomic quantum efficiency , E is energy level

Is quite high (~45%). Thus a large portion of the input power can be converted into useful laser power. Output powers of several watts to several kilowatts can be obtained from CO_2 lasers. This property, together with ease of operation at high power levels in both CW and pulsed configurations, has made the CO_2 laser widely applicable as a source in the laser processing of materials. High-power CO_2 lasers find applications in materials processing, welding, hole drilling, cutting, etc., and because of their very high output power. In addition, the atmospheric attenuation is low at 10.6 μm which leads to some applications of CO_2 lasers in open air communications.
(K. Thyagarajan. Ajoy Ghatak 2010).

2-4 Effect of Temperature

Like all other semiconductor devices, solar cells are sensitive to temperature. Increases in temperature reduce the band gap of a semiconductor, thereby effecting most of the semiconductor material parameters. The decrease in the band gap of a semiconductor with increasing temperature can be viewed as increasing the energy of the electrons in the material. Lower energy is therefore needed to break the bond. In the bond model of a semiconductor band gap, reduction in the bond energy also reduces the band gap. Therefore increasing the temperature reduces the band gap.

CHAPTER THREE

EXPERIMENTAL PART

This chapter presents the experimental part of this work, setup arrangement and experimental procedure.

3-1 Experimental setup

The setup used to study the IV characteristics curve of the modified solar cell is shown in figure (3.1a) below as schematic diagram and the photograph of the arrangement of this setup is shown in figure (3.1b).

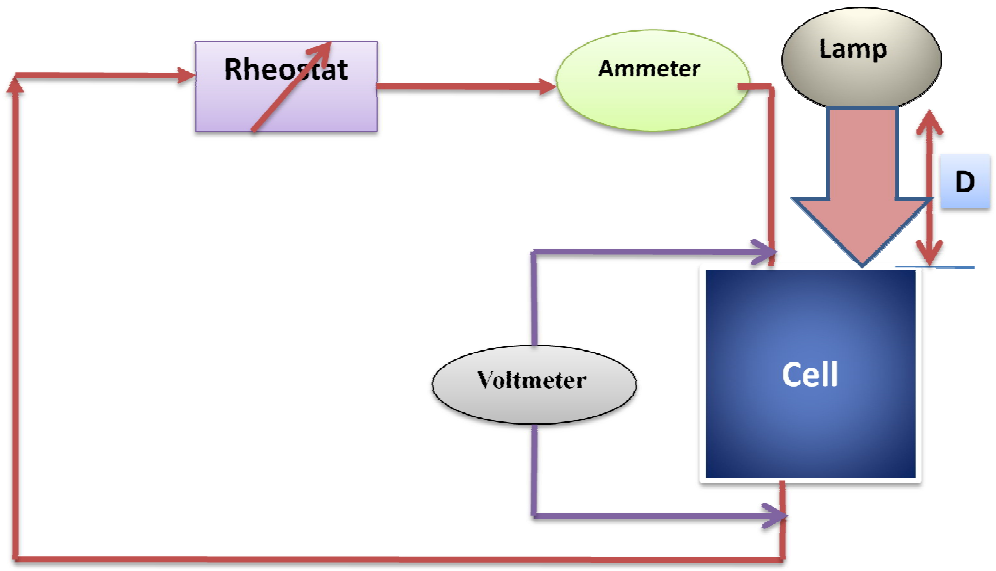

Fig (3.1a): Experimental Setup for Solar cell (with & without surface texture) IV curve Measurements.

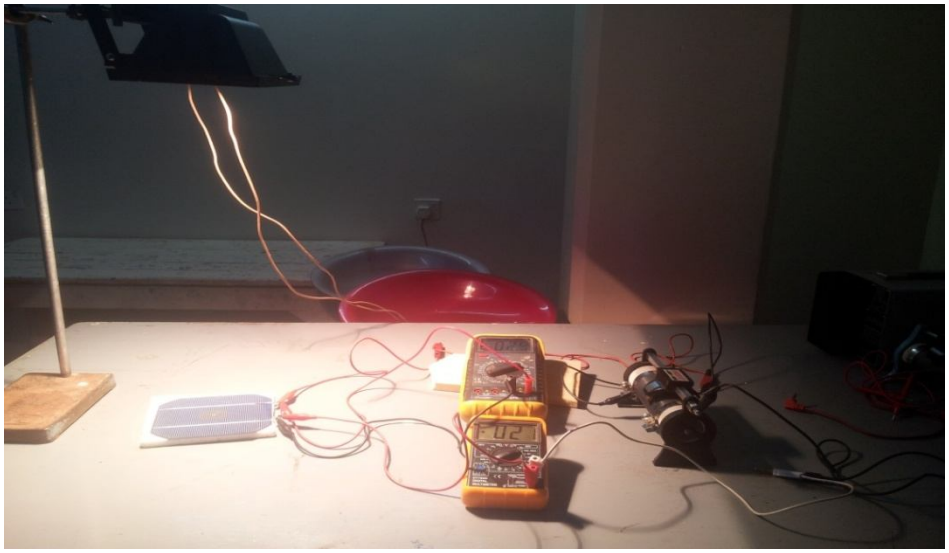

Fig (3.1b): **setup arrangement to measure I-V characteristic of solar cell.**

The main part of this setup is the silicon solar cells, those are assembled by San Fu Chemical Company, Chung Shan, and Taipei, Taiwan with specifications listed in table (3.1). And Figure (3.2) below shows the cell. (austinsolartech.2015)

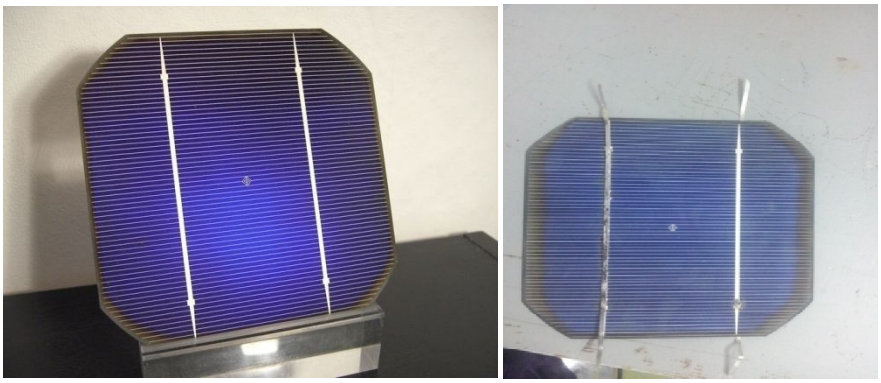

Fig (3.2): 125x125mm mono-crystalline solar cells

Table(3.1): **Solar cells samples specifications**

Properties	Value
Size	125*125mm ±1mm (5 inch)
Efficiency	17.2%
Thickness (Si)	240 μm +/- 40 μm
Busbar quantity	2
Color	nice uniformity blue color
Front	Blue silicon nitride anit-reflection coated.

	1.5mm silver busbar
Max power	2.505~2.535 Watt
Diagonal:	150 mm± 1.0 mm (round chamfers)
Based Material	P-type mono-crystalline silicon wafer doped with boron
Back	Surface Aluminum back surface field. 3mm wide segment soldering pads (Silver).
I_{mpp} (A)	4.824
I_{sc} (A)	5.163
V_{pm} (V)	0.525
V_{oc} (V)	0.628

In this work I used (Plus line S 500W R7s 230V 1CT) lamp from PHILIPS as an artificial light source. (Fig 3.3) shows the lamb and its Floodlights (Philips 2015).

Fig (3.3): **Plus line S 500W R7s 230V 1CT Lamb and his Flood light**

Table (3.2) below shows their specifications:

Table (3.2) Lamp commercial & electric's specifications:

Properties	Value
Lifetime (hours)	2000 hr
Luminous Efficacy Lamp	19.3 Lm/W
Lamp Wattage	500 W
Voltage	230 V
Lamp Current	2.17 A

Dimensions	112.6 (min), 114.2 (nom), 115.8 (max)

The device used to measure the intensity of radiant energy was Radiometer/Photometer. It can be defined as an instrument for measurement of visible light luminance. The basic difference between radiometer and photometers is that latter must respond to light as the CIE standard observer.

Radiometer used in this work was assembled by EG&G Company (USA) Model 450-1.Power220V/50Hz, figure (3.4) below shows the radiometer that we use. (Konica Minolta.2015)

Fig (3.4): 450-1 photometer

Also used variable rheostat (40Ω) three terminals, DT-700D digital multimeter as Ammeter and Voltmeter and CO_2 (130W) laser.

3-2 I-V Characteristic curve Investigation

The apparatus were connected as shown in Fig (3.1), the distance (D) from the lamp to the solar cell was carefully measured and control during all measurements = 39.5cm, solar cell without laser irradiation was used firstly and read its voltage and current which controlled by rheostat ,the obtained results were tabulated and plotted. Solar cell fill factor were calculated according to: $FF = \frac{I_m V_m}{I_{sc} V_{oc}}$, and the efficiency was estimated from this values.

The procedures above were repeated with solar cell of single area of irradiation. The results of IV characteristics curve of the solar cell without irradiation and with irradiation was compared. The effect of irradiations on solar cell parameters was studied and compared. Effect of irradiation on cell efficiency was studied.

3-3 Treatment with Laser

Laser used in this work was CO_2 laser (130W) manufactured by China with specifications listed in table (3.3). (recilaser.2015)

Table (3.3) Co_2 laser commercial specification which manufactured by Bei jing laser technology Co., Ltd.

Properties	Value
Tube model	S6
Power supply model	P16
Laser-type	10.6μm CO_2 glass laser tube / water-cooling
Ignition voltage	28kv
Laser power	100W/130W
Tube net weight	5kg
Tube length	1650mm
Efficiency	89%
Operating temperature	2 – 40℃
Operating humidity	10-60%
Maximum current	32mA
Graphic format supported	HPGL, BMP, PLT, DST, DXF, and AI
Cooling mode	Purified water: 3 to 5 liter/minute. Water temperature:10℃-40℃.
Auxiliary equipments	Exhaust-fans, air-exhaust pipe, air pump, water pump
Controller	DSP

And CNC table which shown in figure (3.5). to control the direction and speed of laser light which used in this work (A CNC router is a computer controlled cutting machine related to the hand held router used for cutting various hard materials, such as wood, composites, aluminum, steel, plastics, and foams. CNC stands for computer numerical control).

This laser machine takes CO_2 laser tube as thermal source, it can engrave and cut, thus it is applicable for various industries. So it can realize high efficiency and good quality processing effect for various industries. (recilaser. 2015)

Fig (3.5): CNC table for CO_2 engraving & cutting application.

Figure (3.6) shows how Laser beam delivered to working area by using reflection silvered mirrors and a lenses made from quartz (15mm) focal length to focus laser spot size .and diode (630nm) as aiming beam.

Fig (3.6): Technique of deliver laser beam to working area by mirrors.

Parameters of laser treatment were adjusted and assumed to take the following values: maximum output power (P = 27W), Pulse duration = 200μs, Frequency (υ) =5 KHz. And the textured area is 9cm^2. The texture consisting of parallel points of molten silicon with spacing of 40μm was produced.

*All treatments and measurements have been done at room temperature.

CHAPTER FOUR

RESULTS AND DISCUSSION

In this chapter the experimental result of one sample investigated solar cells which irradiated by 10.6 µm, 27W laser radiation, are presented and compared with the origin manufactured. The results are divided into two groups; before and after illumination with laser, In order to show the effect of texturing on the voltage and current.

4-1 I-V Characteristic Curve Results

4-1-1Before Irradiation

Table (4.1) lists voltage and current density values for sample which do not irradiated by laser. The first column represents the voltage by unit (volt) whish changes with variation of resistance value. The second column shows the value of current density by unit (milli ampere per centimeter square) which changes according to voltage changes.

Table (4.1) List of voltage /current density value before irradiation

V(Volt)	I(mA/cm^2)
0.37	**1.6**
0.40	**1.6**
0.41	**1.6**
0.42	**1.5**
0.43	**1.4**
0.44	**1.3**
0.44	**1.2**
0.45	**1.0**
0.45	**0**

Figure (4.1) shows the plot between voltage and current density values for sample which do not irradiated by laser. The X axis represents the voltage by unit (volt). The Y axis represents the values of current density by unit (milli ampere per centimeter square).

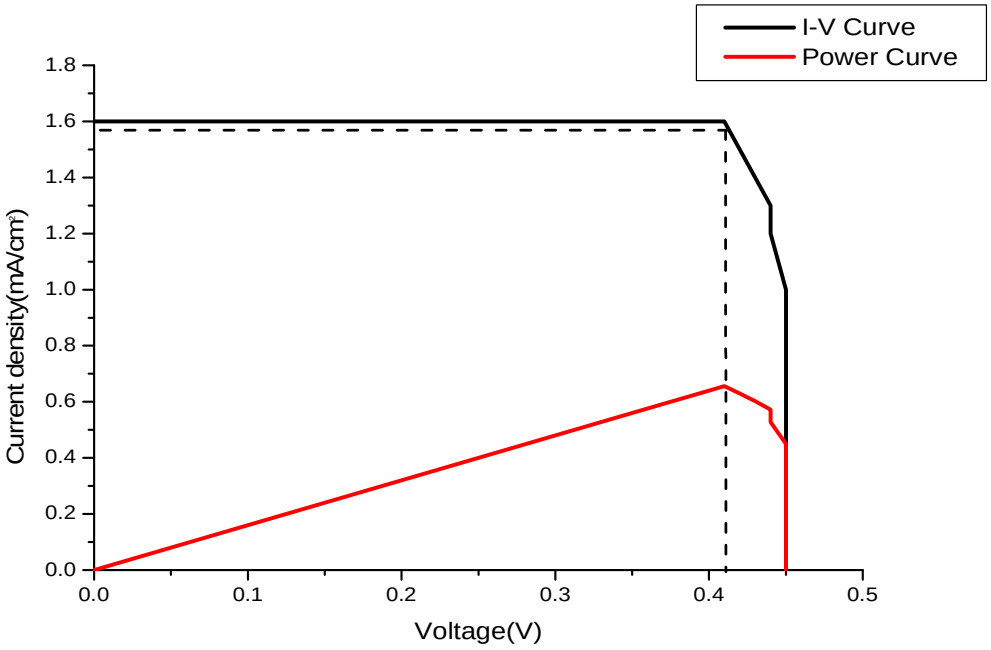

Fig (4.1) plot of the I-V characteristics for cell before irradiation

4-1-2 after Irradiation

Table (4.2) lists voltage and current density values for sample which irradiated by laser. The first column represents the voltage by unit (volt). The second column shows the value of current density by unit (milli ampere per centimeter square).

Table (4.2) List of voltage /current value after irradiation

V(Volt)	I(mA/cm^2)
0.37	**2.3**
0.4	**2.3**
0.41	**2.3**
0.42	**2.3**

0.43	**2.1**
0.45	**1.8**
0.45	**1.5**
0.45	**1.3**
0.45	**1.3**

Figure (4.2) shows the plot between voltage and current density values for sample which irradiated by laser. The X axis represents the voltage by unit (volt). The Y axis shows the values of current density by unit (milli ampere per centimeter square).

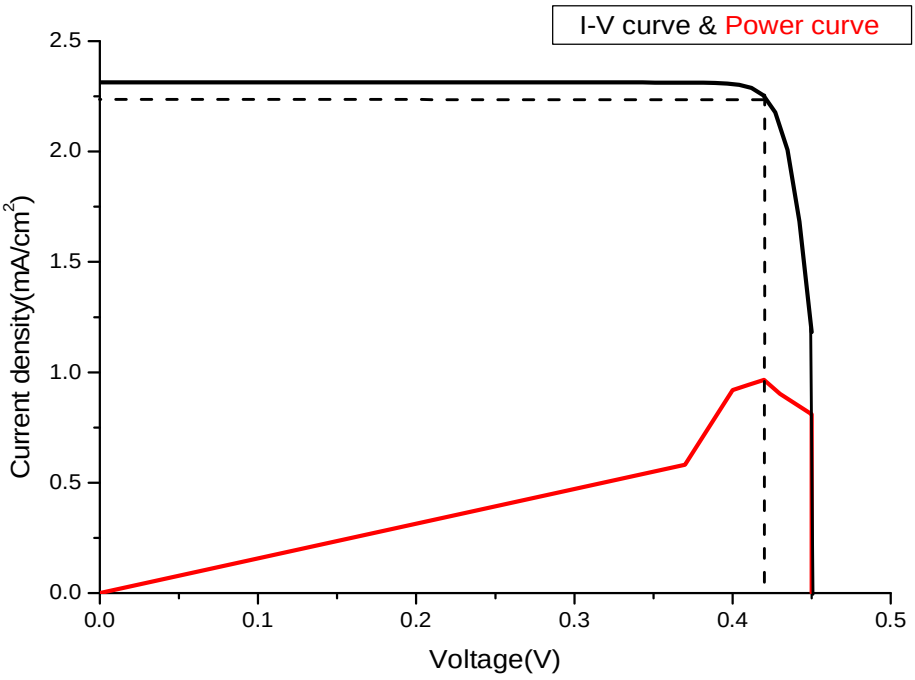

Fig (4.2) plot of the I-V characteristics for cell after irradiation

4-2 Irradiation with Co_2 Laser (10.6µm)

When take look on laser textured wafers revealed that grooves are irregular in shape with positive ridges at both rims. This is the result of interaction of laser beam with the treated surface. Fig (4.3) shows the textured area on the cell which appeared darker than the untextured area.

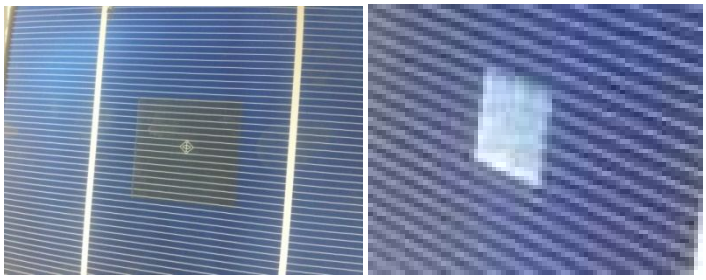

Fig (4.3): textured area on the cell

Fig (4.4) shows the changes in I-V characteristics for cell before and after texturing.

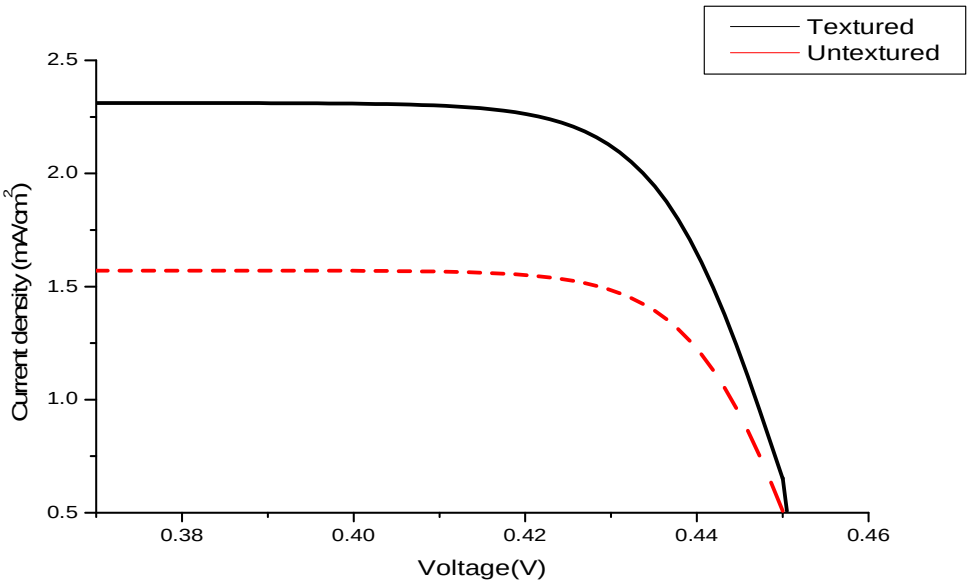

Fig (4.4) Plot shows the changes in I-V characteristics for cell before and after texturing.

By take the $V_{oc,}$ I_{SC},I_{max} and V_{max} from each graph we can calculate fill factor and then efficiency by used equations (2.8) and (2.12) . The value of light intensity from distance equal to 39.5 cm was 0.386 Watt/m^2 and the cell area equal to 0.015625 m^2.

Table (4.3) shows the electrical properties for cell before and after irradiation:

Table (4.3) electrical properties for each cell before and after irradiation

Type of Solar cell	Voc (Volt)	Isc (mA)	Imax (mA)	Vmax (Volt)	FF%	η %
Untextured cell	0.45	1.56	1.6	0.41	0.88	10.5%
Laser textured cell	0.45	2.311	2.24	0.42	0.9046	15.6%
Increase by percentage	0%	75.1%	64%	1%	2.4%	~ 50%

4-3 Discussion

Irradiation the samples with CO_2 laser (10.6μm) resulted in an increase in Short Circuit Current (I_{sc}) magnitude. Consequently noticed increase in I-V curve. When plotted a rectangle on the graph there was changed in the maximum Current, maximum Voltage and Fill Factor magnitude.

As a comparison with another study was done by using conventional methods of texture the result showed an increasing in the efficiency in less time and perfect results. The efficiency of cell was increased with 50% than before irradiation. And noticed that change the light intensity incident on a solar cell changes all solar cell parameters, including the short-circuit current, the open-circuit voltage, the FF, the efficiency and the impact of series and shunt resistances

4-4 Conclusions

In this study, some of the versatile capabilities of laser processing to modify the surface properties of materials. In order to enhance their performance for variety of application. Textured surface was obtained on conventional monosilicon photovoltaic's cell by carbon dioxide laser (10.6μm).

Images show a semi periodic structure known as ripples in the micrometer ranges. The results in this work showed that the use of laser is good method to enhance the efficiency of solar cell by allow trapping more light inside it.

Laser surface treatment introduces defects into the top layer of processed material that deteriorate performance of the solar cell. Fortunately, applied post-laser texturing etching step makes it possible to remove distorted layer and improve efficiency of corresponding solar cells.

4-5 Future work

Usage of CO_2 laser with a different power and different repetition rate to increase the efficiency. Or another type of laser source. Or may change the type of cell by poly silicon type instead of mono silicon. Further studies can be done by investigate another optical or electric phenomena.

References

Ali A. S. Marouf et al. (2014) *the role of photonic processed Si surface in Architecture Engineering*. Vol (1) USA. Study of Civil Engineering and Architecture (SCEA).

A.M Taleb, et al.(2011) *Nanostructure Formation in Silicon Photovoltaic Cells by Femtosecond Laser Pulses* . Materials Science Forum Vol.670 pp 118-12.

ANTANAS VINČIŪNAS.et,al, al. (2013) Journal of Laser Micro/Nanoengineering: *Effect of Laser Patterning on Properties of Crystalline Si Photovoltaic Cells and Substrates*. Vol. 8, No. 3. Center for Physical Science and Technology. Vilnius, Lithuania

AUSTINSOLARTECH.(2015). *125x125 mono-crystalline solar cells*. [Online] available from: http://www.austinsolartech.com/125x125-solarcell.pdf. [Accessed: august 2015].

Chemistry explained. (2015) Foundations and Applications. *solar cells*. [Online] available from: http://www.chemistryexplained.com/Ru-Sp/Solar-Cells.html. [Accessed: 5th august 2015].

Christiana Honsberg and Stuart Bowde. (2015)*Surface Texturing*. [Online] available from: http://www.pveducation.org/pvcdrom/design/surface-texturing. [[Accessed: 27th july2015]

Christiana Honsberg and Stuart Bowden. (2013) *Formation of a PN-Junction*. [Online] availablefrom:http://www.pveducation.org/pvcdrom/pn-junction/formation-pn-junction. [Accessed: 6th august 2015].

Chriswaterguy's bot ;et-al (2011). *Laser surface texturing*. [Online] available from: http://www.appropedia.org/Laser_surface_texturing. [Accessed: 3rd august 2015].

D.A. Zuev.et.al.(2012)Advanced Laser Technologies : *APPLICATION OF LASER TEXTURING METHOD FOR MC-SI SOLAR CELLS FABRICATION*.2-6 September 2012 ,Thun . Switzerland. Institute on Laser and Information Technologies of the Russian Academy of Sciences, Moscow

G. Bunea ,et.al. *Low Light Performance of Mono-Crystalline Silicon Solar Cells.* In: 4th World Conference on Photovoltaic Energy Conference. 4th World Conference on

Photovoltaic Energy Conference. Waikoloa,HI;2006.pp.13121314.Availablefrom:http://ieeexplore.ieee.org/xpls/abs_all.jsp?arnumber=4059885&tag=1

Gigahertz Optik. (2015) *Reflection, Transmission, and Absorption*. [Online] available from: http://light-measurement.com/reflection-absorption/.[Accessed on 2015-08-11]

GLOBALMARKET,(2015), *Digital Multimeter DT-700D* .[Online] available from: http://www.globalmarket.com/product-info. [Accessed: august 2015].

J. Thorstensen and S. E. Foss, "*Laser assisted texturing for thin and highly efficient monocrystalline silicon solar cells,"* in Proceedings of the 26th European Photovoltaic Energy Conference, pp. 1628 – 1631, 2011.

J. Thorstensen, S. E. Foss, and J. Gjessing, "*Light-trapping properties of patch textures created using Laser Assisted Texturing,"* Progress in Photovoltaic: Research and Applications, available online, DOI: 10.1002/pip.2335, 2013.

K. Thyagarajan · Ajoy Ghatak,(2010) *Lasers Fundamentals and Applications*. Second Edition.springer.USA

KAIS A. ALNAIMEE.(2011) Iraq Journal Of Applied Physics :*Nano /Micro surface texturing and Enhancing of photovoltaic cells Efficiency by using UV femtosecond laser pulses* .Vol 7 .No 2 .June .National Institute of optical application .Florence .Italy

Konica Minolta.2015 (*Radiometer and photometer*)[Online]available from:http://sensing.KonicaMinoltaasia/learningcenter/lightmeasurment/radiometerphotometers/ (accessed at 8.10.2015)

L.A DOBRZAŃSKI, & DRYGAŁA A.(2008) *Surface texturing of multicrystalline silicon solar cells. Journal of Achievements in Materials and Manufacturing Engineering. By International OCSCO World Press*.(Vol 31 issue1 November).p.77-78

P.Costas, Grigoropoulos, *Transport in Laser Micro fabrication: Fundamentals and Applications*, p (27-31). Cambridge University Press, New York,(2009)

PHILIPS.(2015) *Plusline S 500W R7s 230V 1CT*[Online] available from :

http://www.lighting.philips.com/main/prof/lamps/halogen-lamps/mv-halogen-without-reflector/plusline-small/924735544298_EU/product (accessed: 1st Sep 2015)

RICELASER.(2015)*Beijing Reci Laser Technology Co., Ltd*.[Online] available from: http://www.recilaser.com/en/index.htm. [Accessed: 22 august 2015].

S.Matthew Brown and B.Craig Arnold. (2010) *Fundamentals of Laser-Material Interaction and Application to Multiscale Surface Modification* in: K. Sugioka et al. (eds.), *Laser Precision Microfabrication*. Springer Series in Materials Science 135, DOI 10.1007/978-3-642-10523-4__4, Verlag Berlin Heidelberg

The physics classroom. (1996-2015) *Light Absorption, Reflection, and Transmission*. [Online]Available from: http://www.physicsclassroom.com/class/light/Lesson-2/Light-Absorption,-Reflection,-and-Transmission. [Accessed: 6th august 2015]

Tiwari G. N. and Mishra R. K.(2012) *Advanced Renewable Energy Sources: The Ecofriendly Photovoltaic Thermal (PVT) System will be the Future Electrical and Thermal Energy Power to Achieve Energy Security for Developing/Underdeveloped Countries*. ch(3)P.114.121.125-128. Royal Society of Chemistry, Thomas Graham House .Cambridge.

Wikipedia .the free Encyclopedia. (2015) *Carbon dioxide laser* .[Online] available from : https://en.wikipedia.org/wiki/Carbon_dioxide_laser. (accessed in 1st Sep 2015)

Wikipedia, the free encyclopedia. (2015) *solar cell*. [Online] available from https://en.wikipedia.org/wiki/Solar_cell . [Accessed: 6th august 2015].